J. Chem. Sci. Vol. 129, No. 4, April 2017, pp. 505–513. © Indian Academy of Sciences.
DOI 10.1007/s12039-017-1260-z

REGULAR ARTICLE

DFT study on the mechanism of $InBr_3$-catalyzed [2+2] cycloaddition of allyltrimethylsilane with alkynones

XING HUI ZHANG*
College of Chemical Engineering, Lanzhou University of Arts and Science, Lanzhou, 730010, China
Email: zhxh135@126.com

MS received 7 December 2016; revised 22 February 2017; accepted 5 March 2017

Abstract. Density functional theory calculations at the M06-2X level were done to study the reaction mechanism and regioselectivity for the [2+2] cycloaddition of allyltrimethylsilane with alkynones using $InBr_3$ as the catalyst. The solvent effect was described by the single-point calculations with SMD model in 1,2-dichloroethane. The calculation results prove that the $InBr_3$-catalyzed cycloaddition of allyltrimethylsilane to alkynones takes place through two possible pathways and get selective cyclobutenone products. The reaction involves two main steps: attack of unsaturated carbon atoms of the alkynone by the π electrons of allyltrimethylsilane and a closed-loop process. The process of forming cyclobutenone product of silicon in the 2-position of the ketone group is more favored and the barrier is 15.5 kcal/mol, while the energies for the cyclobutenone of 3-position product are relatively high of 21.2 kcal/mol. In addition, we calculated the catalytic activity of the InX_3(X=Cl, Br, I) catalyst for this cycloaddition. This is a good explanation for the experimental data that $InBr_3$ and InI_3 would be the most effective catalysts.

Keywords. Indium-catalyzed cycloaddition; allyltrimethylsilane; cyclobutenone; DFT.

1. Introduction

Four-membered carbon rings are a class of highly reactive synthetic precursors and intermediates because of the larger ring-strain. They are also present widely in the structural units of natural products and biologically or pharmaceutically active molecules.[1] Cyclobutenones are important compounds because they are prone to ring-opening by electrocyclic reactions having high regioselectivity under heating or shining light conditions.[2] For cyclobutenones, [2+2] cycloaddition of alkynes with alkenes is widely accepted because they are one of the most efficient and direct methods available. For example, the Lewis acid catalysis,[3–10] transition metal catalysis[11–15] or photo-irradiation[16–19] have been widely used for the [2+2] cycloaddition in the last decade. The research interest has focused on the Lewis acid-catalyzed cycloaddition of silicon-substituted alkenes; such as, allylsilanes have been reported for Mukaiyama– and Sakurai–Hosomi-type reactions.[20,21] Subsequent studies have shown that Lewis acid $TiCl_4$-catalyzed [2+2] cycloaddition could take place for only terminal alkynes and allylsilanes.[22–25] Then, the $Sc(OTf)_3$-catalyzed [2+3] cycloaddition reaction of allylsilanes has been reported to form five-membered β-silylenones.[26,27]

However, Okamoto *et al*., recently reported[28] that indium-catalyzed [2+2] cycloaddition reaction of allylsilanes with internal conjugated alkynones leads to selective cyclobutenone formation. According to the experimental results, indium(III) bromide is considered to be the most effective catalyst for the [2+2] cycloaddition at 0°C and gave the major product in 73% yield in $ClCH_2CH_2Cl$ solvent (Scheme 1). Recently, some theoretical studies of cycloaddition reactions are reported.[29–33] We did not find detailed theoretical investigation for the indium-catalyzed [2+2] cycloaddition reported by the Okamoto *et al*. Therefore, based on all the experimental observations given above, we carried out DFT calculations in order to understand the detailed reaction mechanism and regioselectivity.

2. Computational Methods

The geometries and energies of the reaction systems were optimized in the gas-phase using the M06-2X method[34] of DFT.[35] The M06-2X method could give accurate energies to effectively apply to many theoretical studies of metal-catalyzed reactions.[36–40] For the indium and halogen (X=Cl, Br, I) atoms, the basis set of the Stuttgart–Dresden effective core potential (SDD) were selected.[41–45] Polarization functions were added for In, Cl, Br and I.[46,47] The 6-31G (d, p) basis set[48] was used for all other atoms. This basis set combination

*For correspondence

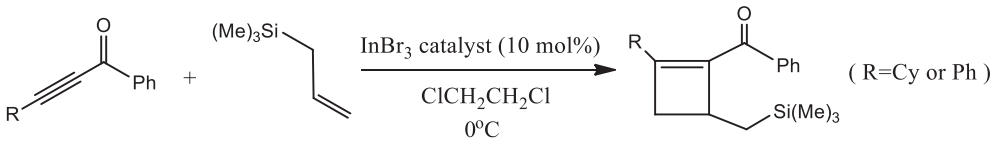

Scheme 1. $InBr_3$-catalyzed [2+2] cycloaddition of allyltrimethylsilane with alkynones.

will be referred to as BS1. Vibrational frequency calculations were done at the same level to identify the transition states or the intermediate structures. The relative energies are corrected for the vibrational zero-point energies (ZPE). The free energies were computed at 298.15 K. The IRC calculations[49,50] were utilized to verify that the transition structure that connected two relevant minima. In order to further obtain more accurate solvation energies from the M06-2X/BS1 results, the single-point energy calculations were done for all the structures using a larger basis set (BS2) in 1,2-dichloroethane by the SMD model at the M06-2X method; the SMD solvation model used the radii and non-electrostatic terms by Truhlar and co-workers.[51] In BS2, the SDD with polarization functions was used for indium and halogen atoms, and ofor ther atoms the 6-311++G(d,p) basis set was used. In this paper, the Gibbs free energies were taken from the M06-2X/BS2//M06-2X/BS1 calculations in dichloroethane unless otherwise stated. All theoretical calculations were performed with the Gaussian 09 program suites.[52]

3. Results and Discussion

For $InBr_3$-catalyzed [2+2] cycloaddition of allyltrimethylsilane with alkynones, we selected a model reaction of $CH_2{=}CHCH_2Si(CH_3)_3$ (labeled as **r**) and PhC(O)CCR (R=Cy or Ph) based on experimental study. The energy profiles for the reaction systems are presented in Figures 1 and 3. The optimized geometries on the potential energy surfaces are shown in Figures 2 and 4, respectively. The relative free energies and the

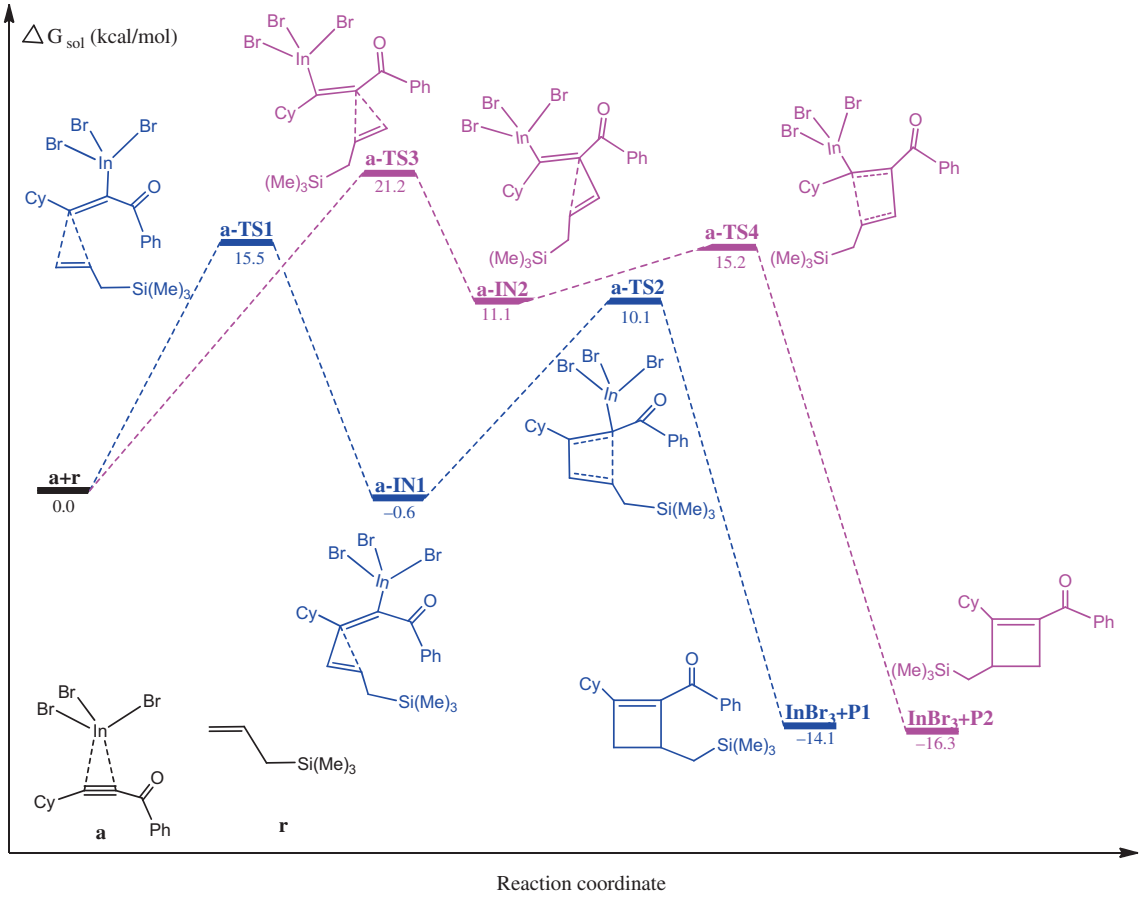

Figure 1. Free energy profiles calculated for the $InBr_3$-catalyzed [2+2] cycloaddition of allyltrimethylsilane r with alkynone (R=Cy).

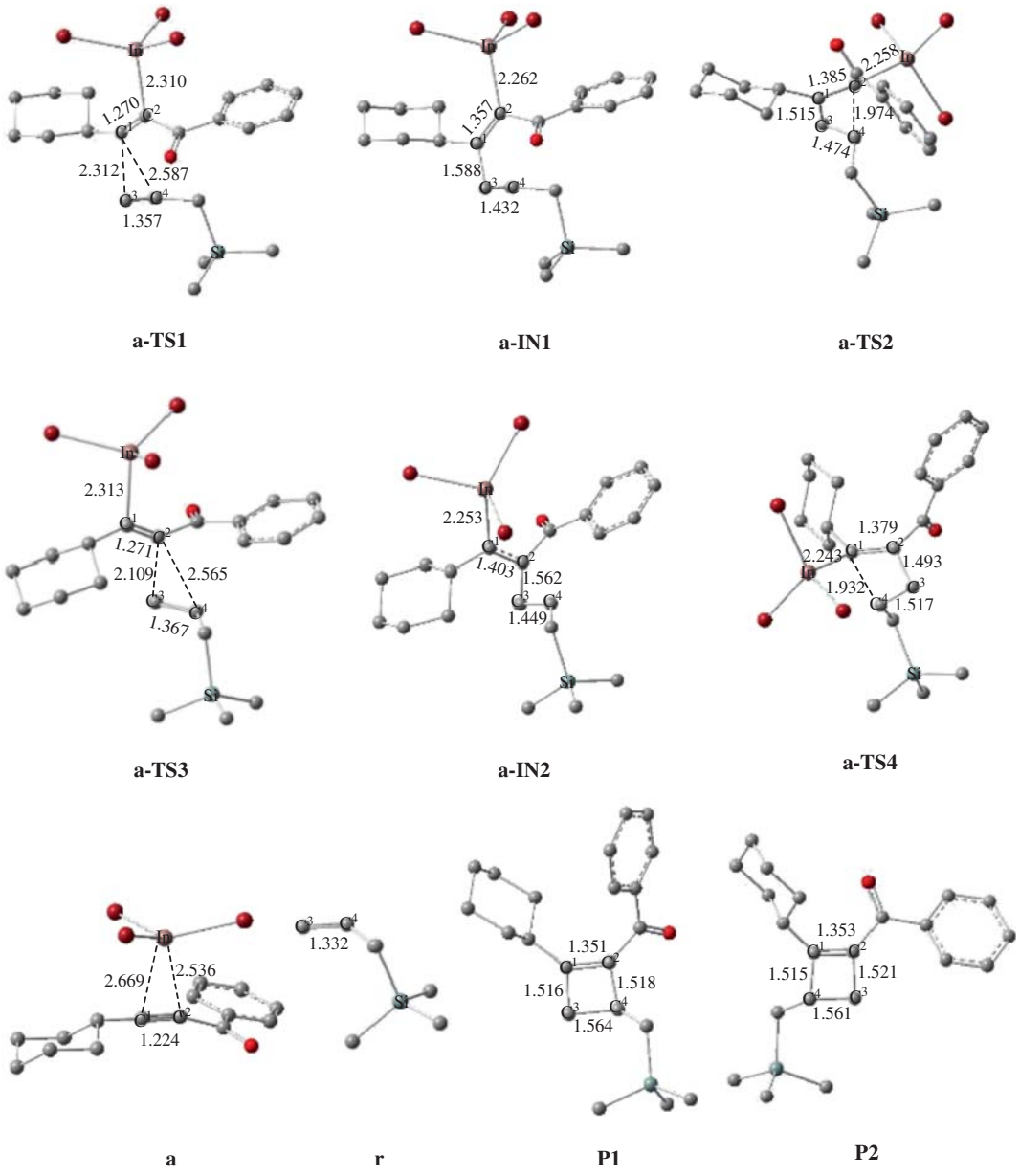

Figure 2. Fully optimized structures of the intermediates and the transition states (shown in Figure 1) with selected bond lengths in Å. The H atoms in structures are omitted for clarity.

activation free energy barriers in the gas and solution phases are shown in Table 1.

3.1 *Pathway a: InBr$_3$-catalyzed cycloaddition leading to cyclobutenone (R=Cy)*

In the Dewar–Chatt–Duncanson (DCD) model,[53] the binding mode of metal σ-donation with π-back-donation and the electronic structure were explored. Once the electrophilic metal complex activated the alkyne, it could be easily attacked by weaker nucleophiles. Therefore, the interaction of the indium atom of $InBr_3$ with the C–C triple bond of alkynone would generate the activated reactant **a**. In the indium complex **a**, the distances of In-C^1 and In-C^2 are 2.668 and 2.536 Å, respectively. The energy profile for the reaction of **a** and **r** (the pathway a) is given in Figure 1. The stationary structures with the selected key parameters of this channel are described in Figure 2. For the reactant molecules **a** and **r**, the intermediate **a-IN1** is given through **a-TS1**. Vibrational analysis shows that the structure **a-TS1** has only one imaginary frequency of 226.8 i cm^{-1}, and IRC confirmed that this TS connects the reactants (**a** and **r**) and intermediate **a-IN1**. Figure 2 shows that C^1 atom of **a** molecule attacks C^3 and C^4 atoms of **r** and the C^1 atom is completely connected with the C^3 atom (the C^1–C^3 and C^1–C^4 bond lengths are 2.312 and 2.587Å, respectively) in **a-TS1**, and the $InBr_3$ molecule transfers

Table 1. The relative free energies and activation free energies in the gas phase and in solution for the structures shown in Figures 1, 3 and 5; the values are given in kcal/mol.

species	ΔG_{gas}	ΔG^{+}_{gas}	ΔG_{sol}	ΔG^{+}_{sol}
a+r	0.0		0.0	
a-TS1	18.5	18.5	15.5	15.5
a-IN1	9.8		−0.6	
a-TS2	14.4	4.6	10.1	10.7
$InBr_3$+P1	−11.5		−14.1	
a-TS3	25.0	25.0	21.2	21.2
a-IN2	12.2		11.1	
a-TS4	16.6	4.4	15.2	3.1
$InBr_3$+P2	−14.0		−16.3	
b+r	0.0		0.0	
b-TS1	16.3	16.3	14.6	14.6
b-IN1	6.2		−3.0	
b-TS2	12.1	5.9	8.8	11.8
$InBr_3$+P3	−15.5		−17.4	
b-TS3	21.8	21.8	21.6	21.6
b-IN2	10.2		9.8	
b-TS4	14.7	7.1	14.4	12.0
$InBr_3$+P4	−15.7		−17.5	
c+r	0.0		0.0	
c-TS1	16.2	16.2	17.1	17.1
c-IN1	7.2		1.6	
c-TS2	11.4	4.2	8.2	6.6
$InCl_3$+P3	−19.9		−26.4	
c-TS3	23.2	23.2	25.1	25.1
c-IN2	8.5		6.8	
c-TS4	13.0	4.5	14.8	8.0
$InCl_3$+P4	−20.0		−26.5	
d+r	0.0		0.0	
d-TS1	15.7	15.7	15.0	15.0
d-IN1	6.5		−1.7	
d-TS2	11.1	4.6	7.6	9.3
InI_3+P3	−12.0		−20.5	
d-TS3	22.5	22.5	23.4	23.4
d-IN2	5.9		2.1	
d-TS4	12.3	6.4	11.5	9.4
InI_3+P4	−12.2		−20.6	

from C^1 to C^2 atom. The transition vector for **a-TS1** is displayed by the C^1 and C^3-C^4. Inspection of Table 1 and Figure 1 shows that the activation free energy for **a-TS1** is 15.5 kcal/mol and the free energy for **a-IN1** is −0.6 kcal/mol with respect to the reactants. In **a-IN1**, the C^1 and C^3 atoms are connected and the bond length is 1.588 Å. Moreover, the C^3 atom has accomplished migration of $sp^2 \rightarrow sp^3$ rehybridization in this step, and the C^3–C^4 has become completely the single bond of length 1.432 Å. The C^1–C^2 bond has lost its triple-bond character and the length is now 1.357 Å. Subsequently, the intermediate **a-IN1** undergoing a closed-loop mechanism results in the final product (**P1**) and regeneration of the catalyst ($InBr_3$) through **a-TS2**. In **a-TS2**, the C^2–C^4 bond distance is 1.974 Å. The activation free energy for the last step is 10.7 kcal/mol, and the whole catalytic process is exothermic by −14.1 kcal/mol. The intermediate **a-IN1** is easy to obtain the product (**P1**) and the catalyst ($InBr_3$). From Figure 1, the first step was found having the higher barrier, this step is also the rate-determining step of the reaction channel.

Alternately, an attack of the C^2 atom onto the C^3–C^4 double bond would be able to get another possible reaction pathway. The energies for this channel are also depicted in Table 1 and Figure 1. The critical structures with the parameters are given in Figure 2. In Figure 1, in the first step, the attack of the C^2 onto the double bond (C^3–C^4) would form the intermediate **a-IN2** through **a-TS3**. The new C^2–C^3 and C^2–C^4 bond distances are 2.109 and 2.565 Å, respectively, in **a-TS3**. The free energy of **a-TS3** is calculated to be 21.2 kcal/mol and the energy for the intermediate **a-IN2** is 11.1 kcal/mol for the reactants **r**+**a**. It is important that this step (**a-TS3**) is also the rate-determining step of the pathway. The higher energies found for **a-TS3** in comparison to **a-TS1** may be due to following reasons: The NBO charges for the C^1, C^2 and C^3 atoms of the reactants (**r**+**a**) are 0.1670, −0.7439 and −0.1051 au, respectively. C^1 atom with a positive charge makes the nucleophilic attack of C^3 more feasible than that on the C^2 atom. The C^2–C^3 bond in **a-IN2** becomes completely formed and the length is now 1.562 Å. Furthermore, the C^3–C^4 bond also achieved the conversion of the double bond to a single bond, and the bond length is 1.449 Å. A subsequent step generates the final product (**P2**) and the catalyst ($InBr_3$) by closed-loop process (**a-TS4**). In **a-TS4**, the C^1–C^4 bond distance is 1.932 Å. The activation energy for this step is 4.1 kcal/mol, and the final step is exothermic by −27.4 kcal/mol. The whole catalytic process for the second pathway is exothermic, −16.3 kcal/mol lower than the reactants.

For two possible channels, the transition states, **a-TS1** and **a-TS3** have higher barriers, which are the rate-determining steps of two different channels for the reactants **r**+**a**. According to the calculated results, **a-TS3** has higher activation energy, while the relatively lower barrier was found for **a-TS1**. Calculations prove that the $InBr_3$-catalyzed [2+2] cycloaddition has good regioselectivity and the major product is cyclobutenone **P1**. The calculated results are in agreement with the experimental data of Okamoto *et al.*[28]

3.2 *Pathway b: $InBr_3$-catalyzed cycloaddition leading to cyclobutenone (R=Ph)*

To obtain better influencing factors of the reaction mechanism, we chose indium alkynone complex **b** *via* alkynyl functionality exchange of the Cy with Ph group. The energy profile for the reaction of **b** with **r** is

depicted in Figure 3. The geometries with the corresponding parameters on the potential surface are given in Figure 4. In pathway b, the first step for the attack of the C^1 or C^2 atom onto the π bond of allyltrimethylsilane gives the structures **b-IN1** and **b-IN2** through the transition structures **b-TS1** and **b-TS3,** respectively. Vibrational analysis shows that the structures **b-TS1** and **b-TS3** have only one each with an imaginary frequency of 235.3 and 282.5 i cm^{-1}. The bond lengths C^1–C^3 and C^1–C^4 are 2.290 and 2.502 Å in **b-TS1** and the C^2–C^3 and C^2–C^4 distances are 2.325 and 2.524 Å in **b-TS3**. As the reaction goes from **b-TS1** and **b-TS3** to **b-IN1** and **b-IN2**, the C^1–C^3 and C^2–C^3 bonds are completely formed (1.579 and 1.561 Å). As could be seen from Figure 3, the activation free energy barrier for this step is 14.6 kcal/mol through **b-TS1** and 21.6 kcal/mol for route passing through **b-TS3**. The first step is the rate-determining step for the pathway b and lower barriers were found for **b-TS1** in comparison to those for **a-TS1**. On the last step, the intermediates **b–IN1** and **b-IN2** undergo closed loop process through **b-TS2** and **b-TS4** and get the final products **P3** and **P4**, and release the catalyst $InBr_3$. The energies of activation were calculated to be 11.8 and 12.0 kcal/mol for **b-TS2** and **b-TS4** to release the products and regenerate the catalyst. In addition, the whole catalytic cycle is also exothermic and the energies are −17.4 and −17.5 kcal/mol, respectively. The lower barrier is found for the channel marked in blue line and the pathway of **b+r→b-TS1→b-IN1→b-TS2→P3+InBr$_3$** is favorable.

3.3 *The reactivity of the catalyst InX$_3$(X=Cl, Br, I)*

In view of the original experimental results, in order to further explore the catalytic activity of the indium catalyst, we selected InX_3(X=Cl, Br, I) as the catalyst and studied the cycloaddition reaction mechanism of allyltrimethylsilane and alkynone. Following the original model and proposed mechanism, similar reaction pathways, c and d were found for the catalysts InX_3(X=Cl and I).[28]

The calculated relative stabilization energies of the catalysts InX_3 (X=Cl, Br, and I) and the alkynone were −10.9, −9.0 and −7.2 kcal/mol, respectively. The reaction pathways c and d were calculated and

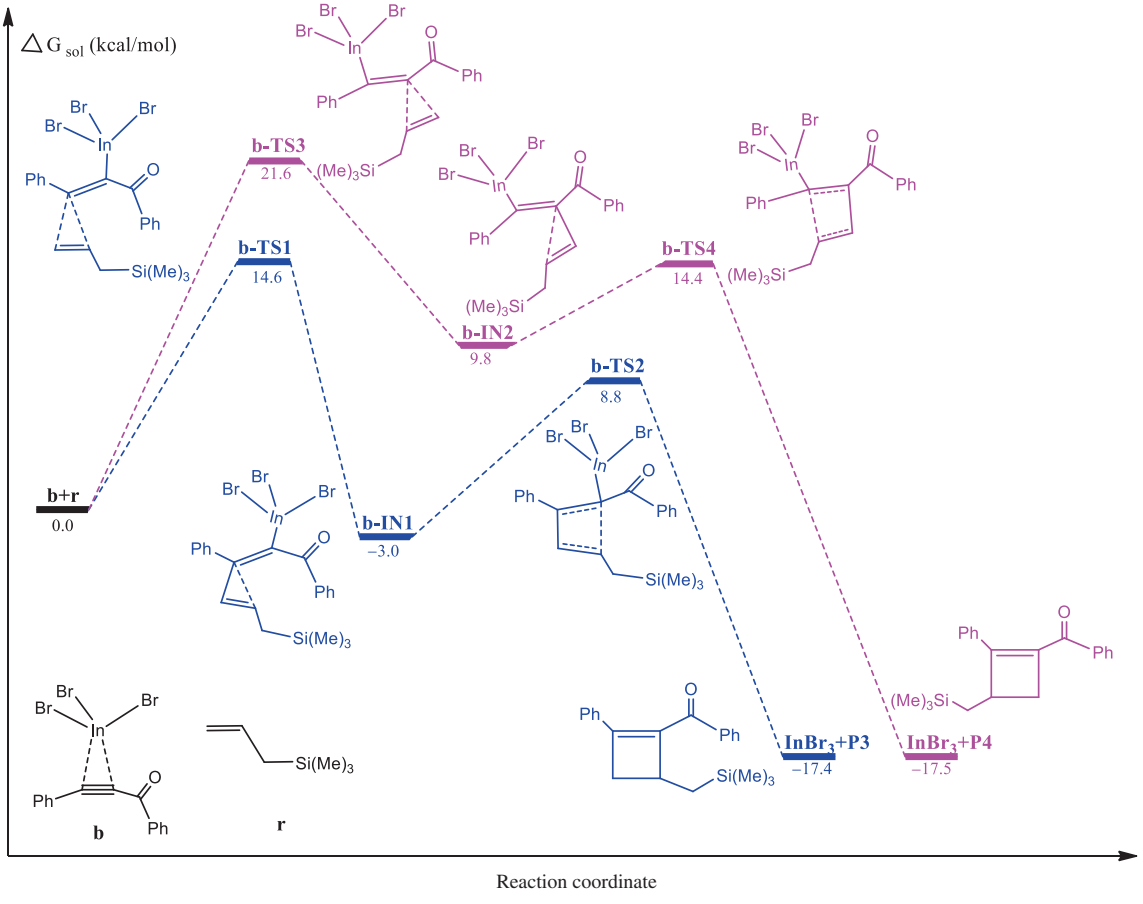

Figure 3. Free energy profiles calculated for the $InBr_3$-catalyzed [2+2] cycloaddition of allyltrimethylsilane r with alkynone (R=Ph).

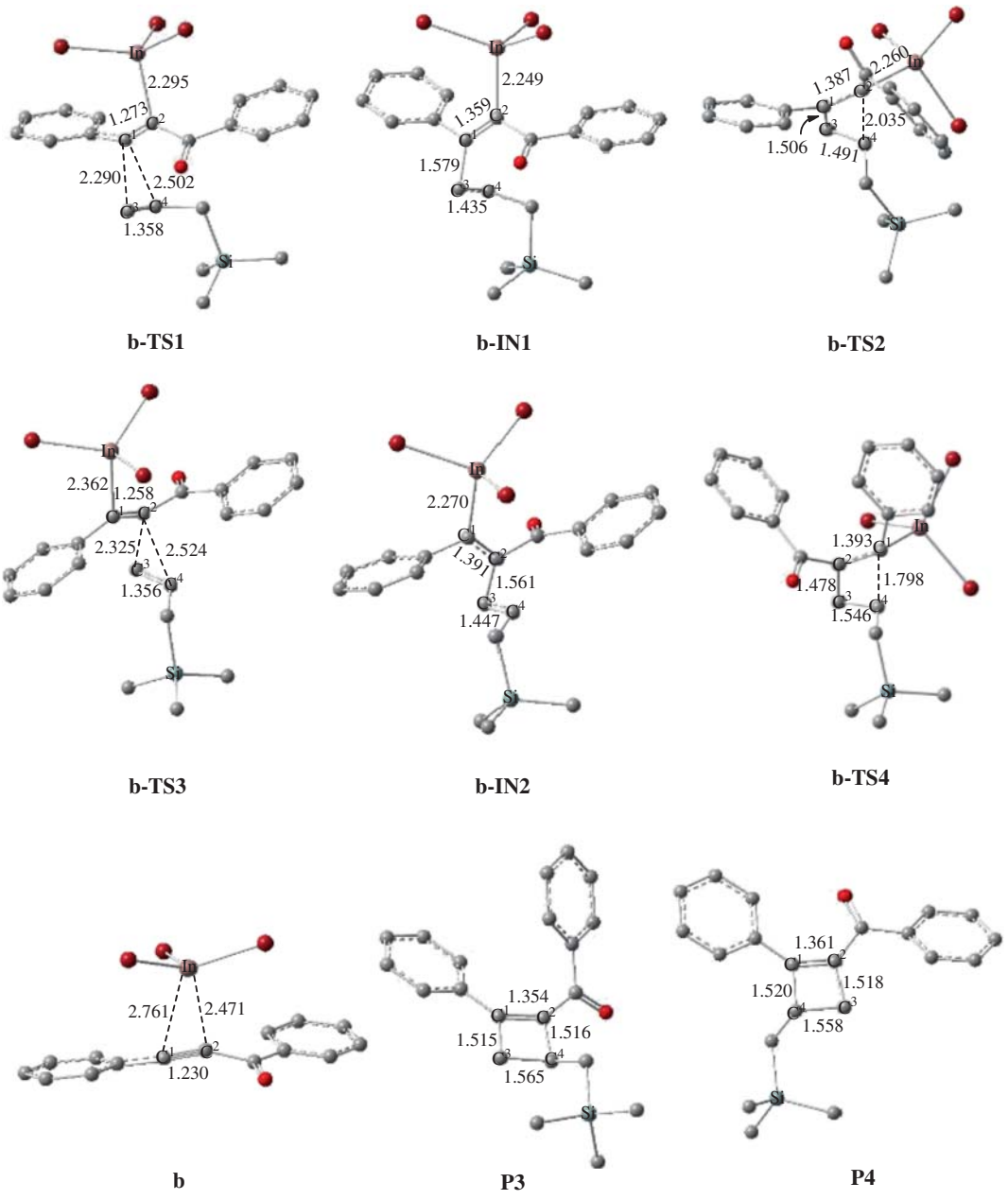

Figure 4. Fully optimized structures of the intermediates and the transition states which are shown in Figure 3, with selected bond lengths in Å. The H atoms in the structures are omitted for clarity.

the energy profiles for of InX_3(X=Cl, Br, I)-catalyzed [2+2] cycloaddition of allyltrimethylsilane to alkynone are shown in Figure 5. The relative energies and the activation free energy barriers in the gas and solution phases are shown in Table 1. The first step is still the rate-determining step of the entire reaction process. According to our calculated results, the activation free energies for **b-TS1**($InBr_3$), **c-TS1**($InCl_3$), **d-TS1**(InI_3) and **b-TS3**($InBr_3$), **c-TS3**($InCl_3$), **d-TS3**(InI_3) are 14.6, 17.1, 15.0 and 21.6, 25.1, 23.4 kcal/mol, respectively. The lower activation free energies found for **b-TS1**, **c-TS1** and **d-TS1** indicate that it is easier for the C^1 atom to attack the π bond of allyltrimethylsilane to generate the corresponding intermediate structure. This path would be the major pathway for product formation. However, higher activation free energies were found for C^2 atom attack of **b**, **c**, **d-TS3**. The energy difference between **TS1** and **TS3** is in the range of 7.0 to 8.4 kcal/mol and show good regioselectivity. For the major product, comparison of activation free energy barriers for pathways b, c and d were found as follows: **c-TS1**>**d-TS1** >**b-TS1**.

Among the three different halogenated catalysts, $InBr_3$ and InI_3 have relatively low activation free energy in consideration of the stabilization energies of the precursor complex. The calculated results show that

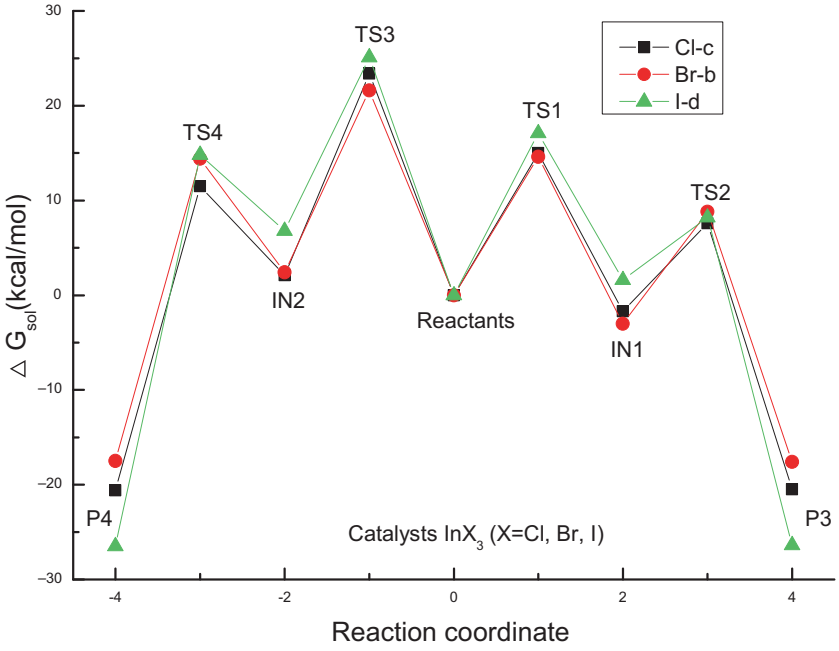

Figure 5. Free energy profiles calculated for the InX_3 (X=Cl, Br, I)-catalyzed [2+2] cycloaddition of allyltrimethylsilane r with alkynone (R=Ph).

$InBr_3$ and InI_3 would be the most effective catalyst for the [2+2] cycloaddition reaction of allyltrimethylsilane to alkynone. In experiments, indium(III) bromide served as the most effective catalyst at 0°C and gave the cycloaddition product in 73% isolated yield, while $InCl_3$ generated 47% yield at 25°C. Thus, the calculated results are consistent with the experimental observations.

4. Conclusions

In this paper, a detailed computational investigation and theoretical estimates were done to find a favorable reaction mechanism for the indium-catalyzed [2+2] cycloaddition of allyltrimethylsilane with alkynones. The calculated results for the studied model ($InBr_3$) showed that the reaction proceeds by two possible pathways and involves two main steps: (1) attack of the unsaturated carbon atoms of the alkynone by the π electrons of the allyltrimethylsilane to form the indium-complex intermediate; (2) a closed-loop process which results in the cyclobutenone product formation and regeneration of the catalyst. For the different reaction channels, the first step is the rate-determining step of the catalytic cycle of cycloaddition. Relatively lower barriers were found for **a-TS1** and **b-TS1** than those of **a-TS3** and **b-TS3**. The major products, P1 and P3 are more easily formed and favored with a lower activation free energy of 15.5 and 14.6 kcal/mol, while the activation barrier for another possible channel is relatively high (21.2–21.6 kcal/mol). The results show that the indium-catalyzed [2+2] cycloaddition has the good regioselectivity and high yield, which is consistent with the experimental observations of Okamoto *et al*. Meanwhile, we calculated the catalytic activity of the InX_3(X=Cl, Br, I) catalyst for this cycloaddition. The reactivity of indium catalysts decreases in the order: $InBr_3 > InI_3 > InCl_3$. This is a good explanation for the experimental results that $InBr_3$ and InI_3 would be the most effective catalyst compared to $InCl_3$.

Supporting Information (SI)

Tables giving Cartesian coordinates for the calculated stationary structures obtained from the DFT calculations are given in Supplementary Information, which is available at www.ias.ac.in/chemsci.

Acknowledgements

This work was supported by Longyuan young creative talents to support projects, Gansu Province (2014-98), and the Natural Science Foundation of Department of Education, Gansu Province (2016B-121). We are grateful to the Gansu Province Supercomputer Center for essential support. We are grateful to the Reviewers for their invaluable suggestions.

References

1. Anslyn E V and Dougherty D A 2006 In *Strain and stability. Modern physical organic chemistry* (Sausalito, CA: University Science Books) p. 65

2. Namyslo J C and Kaufmann D E 2003 The application of cyclobutane derivatives in organic synthesis *Chem. Rev.* **103** 1485
3. Snider B B 1976 The stereospecific aluminum chloride catalyzed [2+2] cycloaddition of propiolate esters with unactivated alkenes *J. Org. Chem.* **41** 3061
4. Snider B B, Brown L A, Conn R S E and Killinger T A 1977 The lewis acid catalyzed reaction of 3-butyn-2-one with alkenes *Tetrahedron Lett.* **18** 2831
5. Fienemann H and Hoffmann H M R 1979 Cyclobutenecarboxylic esters *via* aluminum chloride induced [2+2] cycloadditions of 2-propynoic esters to cyclic olefins *J. Org. Chem.* **44** 2802
6. Snider B B, Rodini D J, Conn R S E and Sealfon S 1979 Lewis acid catalyzed reactions of methyl propiolate with unactivated alkenes *J. Am. Chem. Soc.* **101** 5283
7. Clark R D and Untch K G 1979 [2+2] Cycloaddition of ethyl propiolate and silyl enol ethers *J. Org. Chem.* **44** 248
8. Rosenblum M and Scheck D 1982 Condensation of propiolic esters with olefins catalyzed by the $C_5H_5Fe(CO)_2$ cation *Organometallics* **1** 397
9. Faron K L and Wulff W D 1988 The chromium and tungsten pentacarbonyl groups as reactivity auxiliaries in [2+2] cycloadditions *J. Am. Chem. Soc.* **110** 8727
10. Ishihara K and Fushimi M 2008 Catalytic enantioselective [2+4] and [2+2] cycloaddition reactions with propiolamides *J. Am. Chem. Soc.* **130** 7532
11. Lautens M, Klute W and Tam W 1996 Transition mmetal-mediated cycloaddition reactions *Chem. Rev.* **96** 49
12. Lopez-Carrillo V and Echavarren A M 2010 Gold(I)-catalyzed intermolecular [2+2] cycloaddition of alkynes with alkenes *J. Am. Chem. Soc.* **132** 9292
13. Hilt G, Paul A and Treutwein J 2010 Cobalt catalysis at the crossroads: Cobalt-catalyzed alder-ene reaction versus [2+2] cycloaddition *Org. Lett.* **12** 1536
14. Nishimura A, Ohashi M and Ogoshi S 2012 Nickel-catalyzed intermolecular [2+2] cycloaddition of conjugated enynes with alkenes *J. Am. Chem. Soc.* **134** 15692
15. Sakai K, Kochi T and Kakiuchi F 2013 Rhodium-catalyzed intermolecular [2+2] cycloaddition of terminal alkynes with electron-deficient alkenes *Org. Lett.* **15** 1024
16. Pappas S P, Pappas B C and Portnoy N A 1969 Synthesis and solvolytic rearrangement of 1-methoxybicyclo[4.2.0]octa-3,7-diene-2,5-diones *J. Org. Chem.* **34** 520
17. Serve P and Rosenberg H M 1970 New route to the 2-oxabicyclo[3.2.0]hept-6-ene ring system *J. Org. Chem.* **35** 1237
18. Bloomfield J J and Owsley D C 1971 Photochemistry of acetylenes. I. Photoaddition of ethylene to dimethyl acetylenedicarboxylate *J. Am. Chem. Soc.* **93** 782
19. Koft E R and Smith A B 1984 Intramolecular [2+2] photocyclizations. 2. Total synthesis of (.+-.)-hibiscone C (gmelofuran) *J. Am. Chem. Soc.* **106** 2115
20. Hosomi A 1988 Characteristics in the reactions of allylsilanes and their applications to versatile synthetic equivalents *Acc. Chem. Res.* **21** 200
21. Miura K and Hosomi A 2006 *Allylsilanes, Allenylsilanes, and Propargylsilanes.* In *Main Group Metals in Organic Synthesis* H Yamamoto and K Oshima (Eds.) (Weinheim: Wiley-VCH) p. 489
22. Hojo M, Tomita K, Hirohara Y and Hosomi A 1993 New access to Di-exo-methylenecyclobutanes *via* [2+2] cycloaddition of 3-methylthio-4-trimethylsilyl-1, 2-butadiene with alkenes mediated by a Lewis acid *Tetrahedron Lett.* **34** 8123
23. Monti H, Audran G, Leandri G and Monti J P 1994 ZnI_2 Catalyzed [2+2] versus [3+2] cycloaddition of an allyltrimethylsilane with 3-butyn-2-one: Confirmation of a cyclobutene by-product formation *Tetrahedron Lett.* **35** 3073
24. Inanaga K, Takasu K and Ihara M 2005 A practical catalytic method for preparing highly substituted cyclobutanes and cyclobutenes *J. Am. Chem. Soc.* **127** 3668
25. Takasu K, Hosokawa N, Inanaga K and Ihara M 2006 Cyclobutane ring formation by triflic imide catalyzed [2+2]-cycloaddition of allylsilanes *Tetrahedron Lett.* **47** 6053
26. Okamoto K, Tamura E and Ohe K 2014 Stereoselective construction of 1,3-disilylcyclopentane derivatives by scandium-catalyzed [3+2] cycloaddition of allylsilanes to β-silylenones *Angew. Chem. Int. Ed.* **53** 10195
27. Okamoto K, Tamura E and Ohe K 2013 Acid-catalyzed direct conjugate alkenylation of α,β-unsaturated ketones *Angew. Chem. Int. Ed.* **52** 10639
28. Okamoto K, Shimbayashi T, Tamura E and Ohe K 2015 Indium-catalyzed [2+2] cycloaddition of allylsilanes to internal alkynones *Org. Lett.* **17** 5843
29. Behzadi M, Saidie K, Islami M R and Khabazzadeh H 2016 Experimental and theoretical investigation of benzyl-*N*-pyrrolylketene, one-step procedure for preparing of new β-lactams by [2+2] cycloaddition reaction *J. Chem. Sci.* **128** 111
30. Benallou A, Abdallaoui H A and Garmes H 2016 A conceptual DFT approach towards analysing feasibility of the intramolecular cycloaddition Diels-Alder reaction of triene amide in Lewis acid catalyst *J. Chem. Sci.* **128** 1489
31. Marakchi K, Ghailane R, Kabbaj O K and Komiha N 2014 DFT study of the mechanism and stereoselectivity of the 1,3-dipolar cycloaddition between pyrroline-1-oxide and methyl crotonate *J. Chem. Sci.* **126** 283
32. Wang N N, Tan X J, Wang W H and Li P 2016 Theoretical insights into the cycloaddition reaction mechanism between ketenimine and methyleneimine: An alternative approach to the formation of pyrazole and imidazole *J. Chem. Sci.* **128** 279
33. Tia R, Adei E, Baidoo J and Edor J 2016 Quantum chemical study of the mechanisms of oxidation of ethylene by Molybdyl and Tungstyl Chloride *J. Chem. Sci.* **128** 707
34. Zhao Y and Truhlar D G 2008 The M06 suite of density functionals for main group thermochemistry, thermochemical kinetics, noncovalent interactions, excited states, and transition elements: Two new functionals and systematic testing of four M06-class functionals and 12 other functionals *Theor. Chem. Acc.* **120** 215
35. Parr R G and Yang W 1989 In *Density-functional Theory of Atoms and Molecules* (New York: Oxford University Press)

36. Ajitha M J and Huang K W 2016 Mechanism and regioselectivity of Rh(III)-Catalyzed intermolecular annulation of aryl-substituted diazenecarboxylates and alkenes: DFT insights *Organometallics* **35** 450
37. Wei X X, Fang R and Yang L Z 2015 Mechanism of N-heterocylic carbene-catalyzed annulation of allenals with chalcones to 3-pyrancarbaldehydes or cyclopentene *Catal. Sci. Technol.* **5** 3352
38. Zhao Y and Truhlar D 2008 Density functionals with broad applicability in chemistry *Acc. Chem. Res.* **41** 157
39. Zhao Y and Truhlar D G 2008 Exploring the limit of accuracy of the global hybrid meta density functional for main-group thermochemistry, kinetics, and noncovalent interactions *J. Chem. Theory. Comput.* **4** 1849
40. Jacquemin D, Perpète E A, Ciofini I, Adamo C, Valero R, Zhao Y, Truhlar D and 2010 On the performances of the M06 family of density functionals for electronic excitation energies Vol. 6, p. 2071
41. Dolg M, Wedig U, Stoll H and Preuss H 1987 Energy-adjusted *ab initio* pseudopotentials for the first row transition elements *J. Chem. Phys.* **86** 866
42. Dolg M, Stoll H, Savin A and Preuss H 1989 Energy-adjusted pseudopotentials for the rare earth elements *Theor. Chim. Acta* **75** 173
43. Schwerdtfeger P, Dolg M, Schwarz W H E, Bowmaker G A and Boyd P D W 1989 Laser-induced fluorescence spectroscopy of NCS in a free jet expansion *J. Chem. Phys.* **91** 762
44. Andrae D, Haeussermann U, Dolg M, Stoll H and Preuss H 1990 Energy-adjusted *ab initio* pseudopotentials for the second and third row transition elements *Theor. Chim. Acta* **77** 123
45. Dolg M, Stoll H and Preuss H 1993 A combination of quasirelativistic pseudopotential and ligand field calculations for lanthanoid compounds *Theor. Chim. Acta* **85** 441
46. Hollwarth A, Bohme M, Dapprich S, Ehlers A W, Gobbi A, Jonas V, Kohler K F, Stegmann R, Veldkamp A and Frenking G 1993 A set of d-polarization functions for pseudo-potential basis sets of the main group elements Al Bi and f-type polarization functions for Zn, Cd, Hg *Chem. Phys. Lett.* **208** 237
47. Ehlers A W, Bohme M, Dapprich S, Gobbi A, Hollwarth A, Jonas V, Kohler K F, Stegmenn R and Frenking G 1993 A set of f-polarization functions for pseudo-potential basis sets of the transition metals Sc Cu, Y Ag and La Au *Chem. Phys. Lett.* **208** 111
48. Rassolov V A, Ratner M A, Pople J A, Redfern P C and Curtiss L A 2001 6-31G* basis set for third-row atoms *J. Comput. Chem.* **22** 976
49. Fukui K 1970 Formulation of the reaction coordinate *J. Phys. Chem.* **74** 4161
50. Fukui K 1981 The path of chemical reactions - the IRC approach *Acc. Chem. Res.* **14** 363
51. Marenich A V, Cramer C J and Truhlar D G 2009 Universal solvation model based on solute electron density and on a continuum model of the solvent defined by the bulk dielectric constant and atomic surface tensions *J. Phys. Chem. B* **113** 6378
52. Frisch M J *et al.*, 2009 *Gaussian 09*, revision A.01; Gaussian, Inc.: Pittsburgh, PA.
53. Chatt J and Duncanson J A 1953 Olefin co-ordination compounds. Part III. Infra-red spectra and structure: Attempted preparation of acetylene complexes *J. Chem. Soc.* **3** 2939